

Structure and interaction of flexible dendrimers in concentrated solution

S. Rosenfeldt, M. Ballauff

Physical Chemistry I, University of Bayreuth, 95440 Bayreuth, Germany

P. Lindner

Institut Laue-Langevin, B.P. 156X, 38042 Grenoble Cedex, France

L. Harnau*

*Max-Planck-Institut für Metallforschung, Heisenbergstr. 3, D-70569 Stuttgart, Germany,
and Institut für Theoretische und Angewandte Physik,*

*Universität Stuttgart, Pfaffenwaldring 57, D-70569 Stuttgart, Germany**

(Dated: November 27, 2018)

We study the influence of mutual interaction on the conformation of flexible poly(propyleneamine) dendrimers of fourth generation in concentrated solution. Mixtures of dendrimers with protonated and deuterated end groups are investigated by small-angle neutron scattering up to volume fractions of 0.23. This value is in the range of the overlap concentration of the dendrimers. The contrast between the solute and the solvent was varied by using mixtures of protonated and deuterated solvents. This allows us to investigate the partial structure factors of the deuterated dendrimers in detail. An analysis of the measured scattering intensities reveals that the shape of the flexible dendrimers is practically independent of the concentration in contrast to the pronounced conformational changes of flexible linear polymers.

I. INTRODUCTION

Dendrimers are macromolecular structures that exhibit a defined tree-like architecture.^{1,2,3,4} Figure 1 displays a flexible poly(propyleneamine) dendrimer of fourth generation. The subsequent units are emanating from a focal unit and a monodisperse macromolecular structure results. In this way, dendrimers combine properties of polymers and colloids³ and may find applications such as contrast agents in magnetic resonance imaging,^{5,6} light-harvesting systems,⁷ and drug-delivery systems.^{8,9}

Up to now, the spatial structure of dendrimers is fully understood in the limit of infinite dilution. Figure 1 immediately demonstrates that flexible dendrimers possess a large number of conformational degrees of freedom which follow from rotations about various chemical bonds. Hence, the terminal groups can fold back. As a result of these conformational degrees of freedom, flexible dendrimers adopt a dense core structure (see the discussion in Refs.^{3,10,11,12}). On the other hand, no back-folding of the terminal groups can occur in the case of rigid dendrimers such as polyphenylene dendrimers^{13,14} or stilbenoid dendrimers.¹⁵

Much less is known about the structure and interaction of flexible dendrimers in concentrated solutions. Compared to the huge number of papers on dendrimers in general, only a small number of theoretical^{16,17,18,19,20,21,22,23,24,25,26,27} and experimental studies^{11,28,29,30,31} focus on properties of dendrimers at higher concentrations. Thus, Topp et al.²⁹ studied solutions of poly(propyleneimine) dendrimers (mass fractions between 0.01 and 0.80) by small-angle scattering techniques. They concluded that the size of the dendrimers decreases upon increasing the dendrimer concentration. Bodnar et al.³⁰ conducted small-angle neutron scattering

and rheological measurements at higher concentrations of poly(propyleneimine) dendrimers. These authors suggest dendrimer clustering and interpenetration with increasing concentration. Sagidullin et al.³¹ studied the self-diffusion coefficient of flexible dendrimers up to high volume fractions and obtained the respective scaling exponents.

The first theoretical treatment of the interaction of flexible dendrimers is due to Likos and coworkers.¹⁶ Starting from the Gaussian density distribution of a flexible dendrimer of fourth generation, they demonstrated that the interaction potential $U(r)$ can be directly derived from this density distribution. For not too concentrated solution $U(r)$ has been modeled by a Gaussian in good agreement with experimental data.¹⁷ A significant difference between the measured and the calculated structure factor was only observed at the highest concentration. Goetze et al.²¹ employed monomer resolved computer simulations to examine the significance of many-body effects in concentrated dendrimer solutions. They reported that the effects of many-body forces are small in general and become weaker as the dendrimer flexibility increases. More recently, this problem was re-considered by Terao who performed coarse-grained molecular dynamics simulations of charged dendrimers in aqueous solution in order to clarify the influence of many-body interactions in concentrated solution.^{24,25} Mladek et al.²⁷ showed that amphiphilic dendrimers form clusters of overlapping particles in the fluid, which upon further compression crystallize into cubic lattices with density-independent lattice constants.

Summarizing the work done so far only Ref.¹⁷ has given a quantitative comparison between theory and experiment. It seems fair to say that a comprehensive study of the interaction of flexible dendrimers in concentrated so-

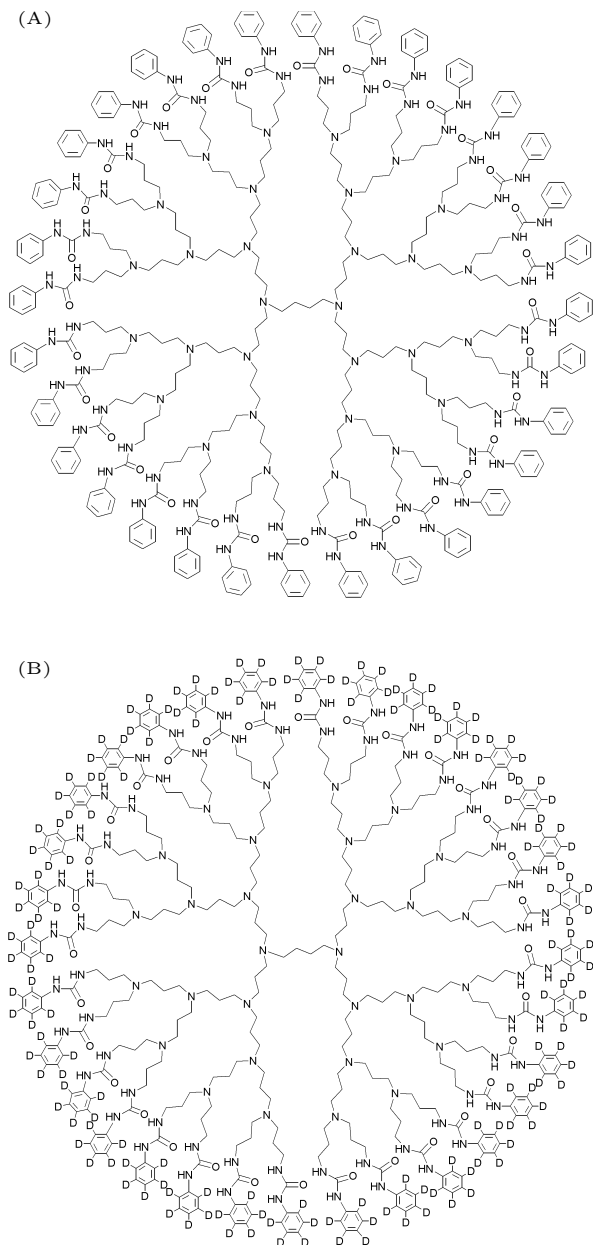


FIG. 1: Chemical structure of the functionalized poly(propyleneamine) dendrimer of fourth generation G4-H having protonated end groups in (A) and the same dendrimer but with deuterated end groups G4-D in (B).

lution is still missing. Moreover, we lack further insight into possible distortions of the structure of flexible dendrimers due to mutual interaction. Many soft materials such as flexible polymers (see, e.g., Refs.^{33,34}), bottle-brush polymers (see, e.g., Refs.^{35,36}), semiflexible polyelectrolytes (see, e.g., Refs.^{37,38}), polyelectrolyte brushes (see, e.g., Refs.^{39,40}), and microgels (see, e.g., Refs.^{41,42}) can be induced to change their shape due to various interactions. Up to now, a similar analysis of possible shape distortions of flexible dendrimers at high concentrations is still missing.

sample	ϕ	ϕ_H	ϕ_D	contrast
S_1	0.15	0.12	0.03	G4-H
S_2	0.15	0.15	0	
S_3	0.23	0.03	0.20	G4-D
S_4	0.23	0.23	0	

TABLE I: Overview of the investigated samples. The volume fractions of the protonated and partially deuterated dendrimers are denoted as ϕ_H and ϕ_D , respectively. $\phi = \phi_H + \phi_D$ is the total volume fraction of the dendrimers. The scattering length density of the solvent (contrast) has been chosen such that samples S_1 and S_3 are investigated at the match point of the G4-H and G4-D dendrimers, respectively.

Here we present a study of the interaction of flexible dendrimers of fourth generation in concentrated solution. As the method, we chose small-angle neutron scattering (SANS).⁴³ Small-angle scattering is the method of choice because it allows us to study the spatial correlations that arise from the excluded volume interactions between the monomers of different dendrimers in the solution. Partially deuterated dendrimers are mixed with the same but protonated dendrimers in dimethylacetamide (DMA) which is a good solvent for this system. As in our previous study of a one-component system¹⁰ contrast variation between the solute dendrimer and the solvent is used by use of mixtures of protonated and the deuterated (DMA). In this way the partial scattering intensities of the deuterated species becomes available. This allows us to investigate both the *structure* and the *interaction* of dendrimers in concentrated solution. In particular, such a study can clearly reveal whether the conformation of dendrimers will be distorted by mutual interaction in concentrated solution.

II. EXPERIMENTAL SECTION

The G4-H dendrimer was synthesized according to Ref.⁴⁴. The specific volume of the G4-H dendrimer was determined to be $\bar{v} = 0.84 \pm 0.01 \text{ cm}^3/\text{g}$ using a DMA-60-densitometer (Paar, Graz, Austria). The partially deuterated dendrimer G4-D was synthesized using fully deuterated phenylisocyanate. The specific volume of the G4-D dendrimer has the value $\bar{v} = 0.82 \pm 0.01 \text{ cm}^3/\text{g}$. Protonated DMA (Fluka, analytical grade) and deuterated DMA (DMA- d_9 , degree of deuteration 99%, Deutero GmbH) were used as received.

We investigated various mixtures of flexible dendrimers of fourth generation with protonated and deuterated end groups by SANS. An overview of the samples is given in Table I, in which we also indicate if the measurements have been performed at the match point of a dendrimer.

The SANS measurements were done using the instrument D11 at the Institut Laue-Langevin. Software provided at the instrument were used to obtain the radial averaged intensities in absolute scale.^{45,46} Further

data treatment was carried out according to literature procedures.^{10,11,15} For all data shown here, the rates of incoherent scattering caused by the protons were determined at high scattering vector, set as a constant and subtracted from the bare data.

III. THEORY

A. Scattering intensity and Ornstein-Zernike equations

SANS determines the scattering intensity $I(\mathbf{q})$ as a function of the scattering vector \mathbf{q} and the concentration of the dissolved particles. In addition to the coherent scattering $I_{coh}(\mathbf{q})$, there is always an incoherent contribution I_{incoh} that is due to the protons present in the particles under consideration. The scattering intensity can be written as

$$I(\mathbf{q}) = I_{coh}(\mathbf{q}) + I_{incoh}. \quad (1)$$

Note that in the notation the dependence on the concentration is suppressed. The \mathbf{q} -independent incoherent contribution I_{incoh} of individual particles must be subtracted carefully from experimental data in order to obtain meaningful results on the structure and interaction of the dissolved particles.¹¹ The systems under consideration are solutions. In view of the mesoscopic scale of the particles, the solvent will be modeled as structureless continuum providing a homogeneous scattering length density.

In general we consider a multicomponent system involving ν species of particles with particle numbers N_H in the volume V . Each particle of a species H ($1 \leq H \leq \nu$) carries n_H scattering units. The coherent contribution to the scattering intensity in the ν -component system is given by

$$I_{coh}(\mathbf{q}) = \sum_{H=1}^{\nu} \sum_{D=1}^{\nu} I_{HD}(\mathbf{q}), \quad (2)$$

with the partial scattering intensities

$$I_{HD}(\mathbf{q}) = \frac{1}{V} \left\langle \sum_{i=1}^{n_H} \sum_{j=1}^{n_D} \sum_{\alpha=1}^{N_H} \sum_{\gamma=1}^{N_D} b_{iH}^{(\alpha)} b_{jD}^{(\gamma)} e^{i\mathbf{q} \cdot (\mathbf{r}_{iH}^{(\alpha)} - \mathbf{r}_{jD}^{(\gamma)})} \right\rangle. \quad (3)$$

Here $\mathbf{r}_{iH}^{(\alpha)}$ is the position vector of the i -th scattering unit ($1 \leq i \leq n_H$) of the α -th particle ($1 \leq \alpha \leq N_H$) of species H . The difference of the scattering length of this scattering unit and the average scattering length of the solvent is denoted as $b_{iH}^{(\alpha)}$, and $\langle \rangle$ is an ensemble average.

It proves convenient to decompose the partial scattering intensities according to

$$I_{HD}(\mathbf{q}) = \tilde{\rho}_H \tilde{\omega}_H(\mathbf{q}) \delta_{HD} + \tilde{\rho}_H \tilde{\rho}_D \tilde{h}_{HD}(\mathbf{q}), \quad (4)$$

where

$$\tilde{h}_{HD}(\mathbf{q}) = \frac{V}{N_H N_D n_H n_D} \times \left\langle \sum_{i=1}^{n_H} \sum_{j=1}^{n_D} \sum_{\alpha=1}^{N_H} \sum_{\substack{\gamma=1 \\ \gamma \neq \alpha}}^{N_D} b_{iH}^{(\alpha)} b_{jD}^{(\gamma)} e^{i\mathbf{q} \cdot (\mathbf{r}_{iH}^{(\alpha)} - \mathbf{r}_{jD}^{(\gamma)})} \right\rangle \quad (5)$$

is a particle-averaged total correlation function for pairs of particles of species H and D . The scattering unit number density of particles of species H is designated by $\tilde{\rho}_H = N_H n_H / V$. The particle-averaged intramolecular correlation function

$$\tilde{\omega}_H(\mathbf{q}) = \frac{1}{N_H n_H} \left\langle \sum_{i=1}^{n_H} \sum_{j=1}^{n_H} \sum_{\alpha=1}^{N_H} b_{iH}^{(\alpha)} b_{jH}^{(\alpha)} e^{i\mathbf{q} \cdot (\mathbf{r}_{iH}^{(\alpha)} - \mathbf{r}_{jH}^{(\alpha)})} \right\rangle \quad (6)$$

characterizes the scattering length distribution, and hence also the geometric shape of particles of species H . While the particle-averaged intramolecular correlations functions account for the interference of radiation scattered from different parts of the same particle in a scattering experiment, the local order in the fluid is characterized by the total correlation functions. In the case of chemically homogeneous particles characterized by $b_H = b_{iH}^{(\alpha)}$, the partial scattering intensities defined in Eq. (4) can be written as

$$I_{HD}(\mathbf{q}) = \tilde{\rho}_H (b_H)^2 \omega_H(\mathbf{q}) \delta_{HD} + \tilde{\rho}_H \tilde{\rho}_D b_H b_D h_{HD}(\mathbf{q}) \quad (7)$$

with $(b_H)^2 \omega_H(\mathbf{q}) = \tilde{\omega}_H(\mathbf{q})$ and $b_H b_D h_{HD}(\mathbf{q}) = \tilde{h}_{HD}(\mathbf{q})$. The total correlation functions $h_{HD}(\mathbf{q})$ are related to a set of direct correlation functions $c_{HD}(\mathbf{q})$ by generalized Ornstein-Zernike equations of the polymer reference interaction site model (PRISM), which in Fourier space read^{47,48,49}

$$h_{HD}(\mathbf{q}) = \sum_{A=1}^{\nu} \omega_H(\mathbf{q}) c_{HA}(\mathbf{q}) (\omega_A(\mathbf{q}) \delta_{AD} + \tilde{\rho}_A h_{AD}(\mathbf{q})). \quad (8)$$

This set of generalized Ornstein-Zernike equations must be supplemented by a set of closure equations. The PRISM integral equation theory has been successfully applied to various experimental systems such as monodisperse ($\nu = 1$) polymers^{35,50,51} and rigid dendrimers,^{15,26} binary mixtures ($\nu = 2$) of charged colloids,^{52,53} three-component mixtures ($\nu = 3$) of charged colloids and salt ions,^{54,55} as well as polydisperse ($\nu \gg 1$) nanoparticles⁵⁶ and polyelectrolyte brushes.⁵⁷

B. Decoupling approximation

A common decoupling approximation is to assume that the conformations of two particles are independent of

each other and of the two mutual positions of their center-of-mass (cm), such that the statistical average in Eq. (5) factorizes. In this case the coherent contribution to the scattering intensity for a binary mixture ($\nu = 2$) is given by

$$\begin{aligned} I_{coh}(\mathbf{q}) &= \rho_H I_H^{(0)}(\mathbf{q}) \left(1 + \rho_H h_{HH}^{(cm)}(\mathbf{q})\right) \\ &+ \rho_D I_D^{(0)}(\mathbf{q}) \left(1 + \rho_D h_{DD}^{(cm)}(\mathbf{q})\right) \\ &+ 2\rho_H \rho_D \sqrt{I_H^{(0)}(\mathbf{q}) I_D^{(0)}(\mathbf{q})} h_{HD}^{(cm)}(\mathbf{q}), \quad (9) \end{aligned}$$

where $\rho_H = N_H/V$ is the number density of particles of species H . The scattering intensity of a single particle of species H reads

$$I_H^{(0)}(\mathbf{q}) = \frac{1}{N_H} \sum_{\alpha=1}^{N_H} \left\langle \sum_{i=1}^{n_H} b_{iH}^{(\alpha)} e^{i\mathbf{q} \cdot \mathbf{r}_{iH}^{(\alpha)}} \right\rangle \left\langle \sum_{j=1}^{n_H} b_{jH}^{(\alpha)} e^{i\mathbf{q} \cdot \mathbf{r}_{jH}^{(\alpha)}} \right\rangle, \quad (10)$$

where the position vector of the i -th scattering unit on the α -th particle of species H is written as $\mathbf{r}_{iH}^{(\alpha)} = \mathbf{R}_H^{(\alpha)} + \mathbf{l}_{iH}^{(\alpha)}$. Here $\mathbf{R}_H^{(\alpha)}$ is the cm position vector of the α -th particle of species H . Spatial pair correlations are characterized by a set of $cm - cm$ total correlation functions

$$h_{HD}^{(cm)}(\mathbf{q}) = \frac{V}{N_H N_D} \sum_{\alpha=1}^{N_H} \sum_{\gamma=1}^{N_D} \left\langle e^{i\mathbf{q} \cdot (\mathbf{R}_H^{(\alpha)} - \mathbf{R}_D^{(\gamma)})} \right\rangle. \quad (11)$$

These total correlation functions are related to $cm - cm$ direct correlation functions by the Ornstein-Zernike relations²²

$$h_{HD}^{(cm)}(\mathbf{q}) = \sum_{A \in \{H, D\}} c_{HA}^{(cm)}(\mathbf{q}) \left(\delta_{AD} + \rho_A h_{AD}^{(cm)}(\mathbf{q}) \right). \quad (12)$$

The $cm - cm$ correlation functions can be expressed in terms of correlation functions between interaction sites by considering the cm as an auxiliary site within the PRISM.^{53,58} Such a relationship provides a direct link between the correlation functions calculated from the PRISM theory and the $cm - cm$ correlation functions which are the basic input into the coarse-graining scheme. In particular the validity of the decoupling approximation can be investigated for particles of arbitrary shape by comparing the calculated scattering intensities with the results of the PRISM.⁵⁸ The decoupling approximation together with the Ornstein-Zernike relation [Eq. (12)] has been successfully applied to monodisperse ($\rho_D = 0$) poly(propyleneamine) dendrimers of the fourth generation¹⁷ although Eqs. (9) - (11) are based on uncontrolled factorization approximations. A computer simulation study²¹ has revealed a breakdown of this factorization approximation at high dendrimer particle number densities similar to earlier findings for flexible polymers based on a comparison with the results for the PRISM.⁵⁸

Starting around the overlap concentration, the following effects are expected: (a) The presence of many dendrimers surrounding a given one leads to a deformation of the dendrimer itself. With increasing concentration the spatial structure of a single dendrimer is expected to deviate more and more from the one given at infinite dilution. (b) Concerning the intermolecular correlations between the dendrimers many-body-correlations become more likely upon increasing the concentration.

IV. RESULTS AND DISCUSSION

The systems under investigation are binary mixtures ($\nu = 2$) of functionalized poly(propyleneamine) dendrimers of the fourth generation with protonated end groups (G4-H) denoted as dendrimers of species H [see Fig. 1 (A)]. The same dendrimers with deuterated end groups (G4-D) are denoted as dendrimers of species D [see Fig. 1 (B)]. All phenyl end groups of the G4-D dendrimers have been fully deuterated to enhance their scattering length as compared to the dendritic scaffold.¹⁰ Note that the overall structure of both dendrimers is identical in the limit $\phi \rightarrow 0$ and the solvent DMA is a good solvent for both systems.¹⁰ Therefore, the intramolecular excluded volume interaction between the monomers significantly influences the shape of the dendrimers.

A. Scattering intensity of single dendrimers

As a prerequisite for studies on the coherent contribution $I_{coh}(\mathbf{q})$ to the scattering intensity at various concentrations, we discuss first the scattering intensities $I_H^{(0)}(\mathbf{q})$ and $I_D^{(0)}(\mathbf{q})$ [see Eqs. (9) and (10)] which have been determined earlier.^{10,11,12} It has been shown that these scattering intensities can be split into three parts according to

$$I_A^{(0)}(q) = \tilde{b}_A^2 I_A^{(S)}(q) + 2\tilde{b}_A I_A^{(SI)}(q) + I_A^{(I)}(q), \quad (13)$$

$$A \in \{H, D\},$$

where $q = |\mathbf{q}|$ and \tilde{b}_A is the so-called contrast, i.e., the difference of the average scattering length density of dendrimers of species A and the scattering length density of the solvent. In the case of SANS, \tilde{b}_A is a parameter that can be varied by mixing protonated and deuterated solvent (contrast variation).¹⁰ The term $I_A^{(S)}(q)$ is the Fourier-transform of a shape function $T_A(r)$ that describes the statistical average over all possible conformations of the dendrimers. This quantity has been compared directly to results of computer simulation studies.^{18,19} The term $I_A^{(I)}(q)$ is related to the scattering length inhomogeneity of the dendrimers, while the term $I_A^{(SI)}(q)$ presents the cross term between the former contributions.¹⁰ For both types of dendrimers (G4-H and

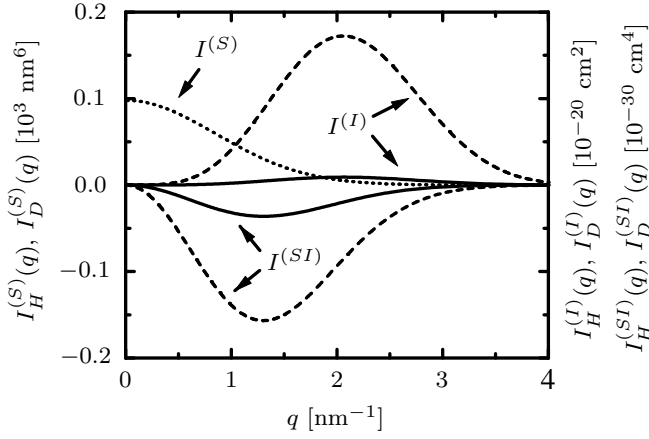


FIG. 2: The partial scattering intensities $I_H^{(I)}(q)$ [$I_H^{(SI)}(q)$] of the G4-H dendrimer (upper [lower] solid line) and $I_D^{(I)}(q)$ [$I_D^{(SI)}(q)$] of the G4-D dendrimer (upper [lower] dashed line) together with $I_H^{(S)}(q) = I_D^{(S)}(q)$ (dotted line) as obtained from modeling scattering data from dilute solution^{10,12} according to Eq. (13). An interpretation of these data leads to the following conclusions: The overall structure of both dendrimers is identical (dotted line), an appreciable number of end groups must fold back into the interior of the dendrimers (dashed lines), and the scattering length distribution is rather homogeneous within in the G4-H dendrimer (solid lines).

G4-D) the shape term $I_A^{(S)}(q)$ can be described by the Gaussian function

$$I_A^{(S)}(q) = V_A^2 \exp\left(-\frac{q^2 R_A^2}{3}\right), \quad A \in \{H, D\}, \quad (14)$$

with the dendrimer volumes $V_H = 9.9 \pm 0.3 \text{ nm}^3$, $V_D = 9.7 \pm 0.6 \text{ nm}^3$, and the radii $R_H = R_D = 1.5 \pm 0.2 \text{ nm}$.^{10,11} Hence the shape function $T_A(r)$ is also a Gaussian function implying that these flexible dendrimers have a dense-core structure.³ For the G4-H dendrimers the terms $I_H^{(I)}(q)$ and $I_H^{(SI)}(q)$ are small as expected for a rather homogeneous scattering length distribution within in the G4-H dendrimers. On the other hand, there is a pronounced difference between the scattering power of the deuterated end groups and the remaining hydrogen atoms in the case of the G4-D dendrimers. Hence, the terms $I_D^{(I)}(q)$ and $I_D^{(SI)}(q)$ are non-negligible due to the inhomogeneous scattering length distribution within in the G4-D dendrimers. Figure 2 shows the partial scattering functions $I_H^{(S)}(q) = I_D^{(S)}(q)$ (dotted line), $I_H^{(I)}(q)$ (upper solid line), $I_D^{(I)}(q)$ (upper dashed line), $I_H^{(SI)}(q)$ (lower solid line), and $I_D^{(SI)}(q)$ (lower dashed line) as obtained from modeling the experimental data.^{10,12} An analysis of the Fourier-transform of $I_D^{(I)}(q)$ allows one to calculate the spatial distribution function of the deuterated end groups of the G4-D dendrimers. Such an analysis has revealed that the end groups are dispersed throughout the dendritic molecule.^{3,10}

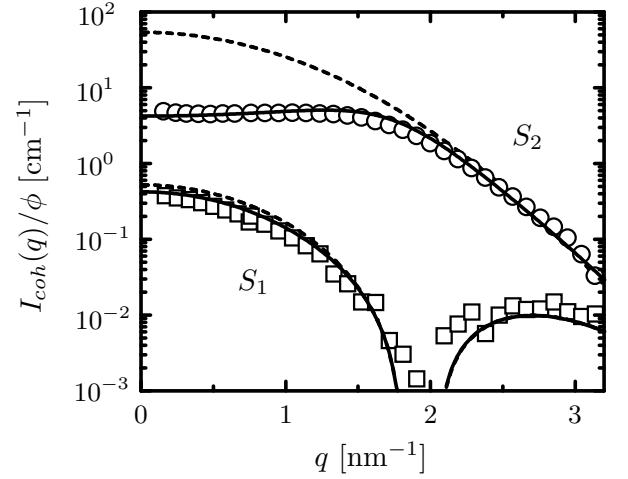


FIG. 3: Experimentally determined scattering intensities $I_{coh}(q)/\phi$ of binary mixtures of G4-H dendrimers denoted as dendrimers of species H [Fig. 1 (A)] and G4-D dendrimers denoted as dendrimers of species D [Fig. 1 (B)] as function of the magnitude of the scattering vector q . For sample S_1 (open squares) the partial volume fractions are $\phi_H = 0.12$ and $\phi_D = 0.03$, while $\phi_H = 0.15$ and $\phi_D = 0$ for sample S_2 (open circles). The scattering intensities have been normalized to the total volume fraction $\phi = \phi_H + \phi_D$ of the dendrimers in the solution. Sample S_1 has been investigated at the match point of the G4-H dendrimers. The solid lines represent the scattering intensity calculated for a solution of interacting dendrimers as obtained from Eq. (17) for sample S_2 and Eq. (18) for sample S_1 . For comparison the dashed lines depict the modeling by Eqs. (17) and (18) with $h_{cm}(q) = 0$.

B. Scattering intensity of interacting dendrimers

Using the scattering intensities of single dendrimers $I_H^{(0)}(q)$ for G4-H and $I_D^{(0)}(q)$ for G4-D [Eq. (13)] as well as the Ornstein-Zernike equations [Eq. (12)], one can calculate the coherent contribution to the scattering intensity $I_{coh}(q)$ for various particle number densities according to Eq. (9). To this end we have solved the Ornstein-Zernike equations together with the hypernetted chain closure

$$\frac{U_{HD}^{(cm)}(r)}{k_D T} = h_{HD}^{(cm)}(r) - \ln\left(h_{HD}^{(cm)}(r) - 1\right) - c_{HD}^{(cm)}(r) \quad (15)$$

and the Gaussian $cm - cm$ interaction potential

$$\frac{U_{HD}^{(cm)}(r)}{k_D T} = N_{HD} \exp\left(-\frac{3r^2}{4R_{HD}^2}\right), \quad (16)$$

where N_{HD} is a model parameter determining the strength of the interaction potential.¹⁷ A Flory-type theory has been used to derive this interaction potential on the basis of the experimentally determined Gaussian functions $I_H^{(S)}(q)$ and $I_D^{(S)}(q)$ given by Eq. (14).^{16,17}

Moreover, the hypernetted chain closure has been found to be in very good agreement with computer simulation data in the case of soft potentials.^{23,32}

Figure 3 displays examples of measured and calculated scattering intensities of a mixture with the total volume fraction $\phi = \phi_H + \phi_D = 0.15$ (see Table I). For the sample S_1 (open squares) the composition is $\phi_H = \rho_H V_H = 0.12$ and $\phi_D = \rho_D V_D = 0.03$. In the case of the sample S_2 (open circles) it is $\phi_H = 0.15$ and $\phi_D = 0$. Sample S_1 has been investigated at the match point of the G4-H dendrimer, i.e., in a solvent where the contrast \tilde{b}_H is zero while $\tilde{b}_D = 1.65 \times 10^{10} \text{ cm}^{-2}$. This contrast variation has been achieved by using mixtures of deuterated and protonated DMA as discussed in Ref.¹⁰. For sample S_2 (only G4-H) the contrast is given by $\tilde{b}_H = -5.02 \times 10^{10} \text{ cm}^{-2}$. The results of the scattering intensities as obtained from Eqs. (9) - (16) with $V_H = V_D = 9.9 \text{ nm}^3$, $R_{HH} = R_{DD} = R_{HD} = 1.4 \text{ nm}$, and $N_{HH} = N_{DD} = N_{HD}$ (solid lines) are in agreement with the experimental data. For comparison, the dashed lines in Fig. 3 depict the modeling of the experimental data assuming a mixture of noninteracting dendrimers characterized by $h_{HH}^{(cm)}(q) = h_{DD}^{(cm)}(q) = h_{HD}^{(cm)}(q) = 0$ in Eq. (9). For the sample S_2 (only G4-H) the steric interaction between the dendrimers that is embodied in the total correlation function $h_{HH}^{(cm)}(q)$ leads to a strong depression of the measured (open circles) and calculated scattering intensity (upper solid line)

$$I_{coh}(q) = \frac{\phi_H \tilde{b}_H^2}{V_H} I_H^{(S)}(q) \left(1 + \frac{\phi_H}{V_H} h_{cm}(q) \right) \quad (17)$$

as compared to the results for noninteracting dendrimers (upper dashed line). Here we have defined the $cm - cm$ total correlation function $h_{cm}(q) \equiv h_{HH}^{(cm)}(q) = h_{DD}^{(cm)}(q) = h_{HD}^{(cm)}(q)$ because $R_{HH} = R_{DD} = R_{HD}$ and $N_{HH} = N_{DD} = N_{HD}$ in Eq. (16). Moreover, we have taken into account that the terms $I_H^{(I)}(q)$ and $I_H^{(SI)}(q)$ are very small for the G4-H dendrimers as already mentioned. The difference between the solid and dashed line in Fig 3 is considerably less pronounced in the case of the scattering intensity of the sample S_1 although the $cm - cm$ total correlation function $h_{cm}(q) = h_{cm}(q, \phi)$ is the same for both samples. For the sample S_1 the intensity is given by

$$I_{coh}(q) = \frac{\phi_D}{V_D} \left(\tilde{b}_D^2 I_D^{(S)}(q) + 2\tilde{b}_D I_D^{(SI)}(q) + I_D^{(I)}(q) \right) \times \left(1 + \frac{\phi_D}{V_D} h_{cm}(q) \right). \quad (18)$$

The contribution of the $cm - cm$ total correlation function $h_{cm}(q)$ is more pronounced for the sample S_2 because the prefactor $\phi_H = 0.15$ in the last term in Eq. (17) is larger than the corresponding prefactor $\phi_D = 0.03$ in the last term in Eq. (18).

Hence, sample S_2 allows one to study the mutual interaction between the dendrimers and the validity of the

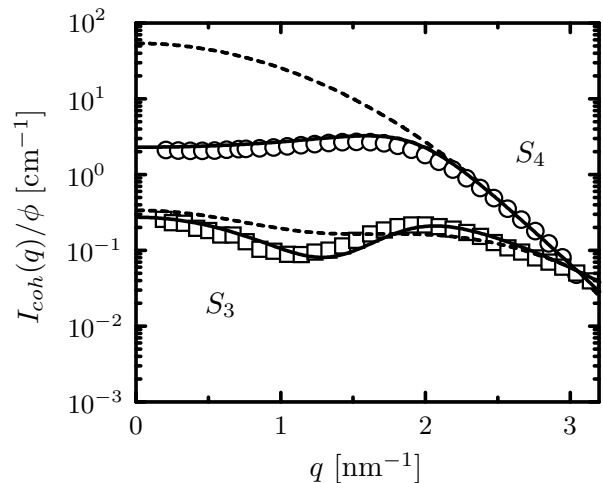


FIG. 4: Experimentally determined scattering intensities $I_{coh}(q)/\phi$ of binary dendrimer mixtures with $\phi_H = 0.03$, $\phi_D = 0.2$ for sample S_3 (open squares) and $\phi_H = 0.23$, $\phi_D = 0$ for sample S_4 (open circles). The scattering intensities have been normalized to the total volume fraction $\phi = \phi_H + \phi_D$. Sample S_3 has been investigated at the match point of the G4-D dendrimers. The solid lines represent the scattering intensity calculated for a dispersion of interacting dendrimers as obtained from Eq. (17) for sample S_4 and Eq. (19) for sample S_3 , while the dashed lines depict the modeling with $h_{cm}(q) = 0$.

$cm - cm$ Ornstein-Zernike equation approach, while the sample S_1 provides nearly direct information about the shape of the dendrimers at high volume fraction. The fact that the calculated scattering intensity (lower solid line) only slightly deviates from the experimental data (open squares) indicates that the shape of the dendrimers is practically independent of the volume fraction $\phi \leq 0.15$ in contrast to pronounced conformational changes of flexible polymers,^{33,34} bottle-brush polymers,^{35,36} and semiflexible polyelectrolytes^{37,38} in semi-dilute solution. For all systems the contribution of the intermolecular interactions to the total free energy increases upon increasing the volume fraction. In order to reduce this contribution a softening of the stiffness of linear macromolecules occurs because for a flexible macromolecule the excluded volume that is not available for the other macromolecules is smaller than the corresponding one of a rigid macromolecule of the same contour length. As a result the size of the macromolecules is reduced considerably upon increasing the volume fraction. For example, the radius of gyration of the bottle-brush polymers studied in Refs.^{35,36} decreases by the factor 1.8 upon increasing the volume fraction from 0.002 to 0.04. In contrast, the flexible and three-dimensional dendrimers under consideration have to be considered as virtually shape-persistent molecules for volume fractions $\phi \leq 0.15$.

Figure 4 displays examples of measured and calculated scattering intensities of a mixture with the total volume fraction $\phi = \phi_H + \phi_D = 0.23$ with $\phi_H = 0.03$, $\phi_D = 0.2$

in the case of the sample S_3 (open squares) and $\phi_H = 0$, $\phi_D = 0.23$ in the case of the sample S_4 (open circles). The total volume fraction of the dendrimers in these samples is comparable to the overlap volume fraction.²¹ Sample S_3 has been investigated at the match point of the G4-D dendrimer, i.e., in a solvent where the contrast \tilde{b}_D is zero while $\tilde{b}_H = -1.65 \times 10^{10} \text{ cm}^{-2}$. For sample S_4 (only G4-H) the contrast is given by $\tilde{b}_H = -5.02 \times 10^{10} \text{ cm}^{-2}$. As before the nearly agreement of the open circles with the results as obtained from the Ornstein-Zernike approach and the decoupling approximation (upper solid line) indicates that the Gaussian $cm - cm$ interaction potential [Eq. (16)] is appropriate even at high volume fractions. In the case of sample S_3 all terms in Eq. (9) contribute to the scattering intensity according to

$$I_{coh}(q) = \frac{\phi_H \tilde{b}_H^2}{V_H} I_H^{(S)}(q) + \frac{\phi_D}{V_D} I_D^{(I)}(q) + \left(\frac{\phi_H}{V_H} \sqrt{\tilde{b}_H^2 I_H^{(S)}(q)} + \frac{\phi_D}{V_D} \sqrt{I_D^{(I)}(q)} \right)^2 h_{cm}(q). \quad (19)$$

The shape of $I_{coh}(q)$ is mainly determined by the functions $I_D^{(I)}(q)$ and $h_{cm}(q)$ characterizing the distribution of the deuterated end groups of the G4-D dendrimers and the intermolecular correlations, respectively, because $\phi_D \gg \phi_H$. The small deviations between the lower solid line and the open squares in Fig. 4 might be either due to slight changes of the distribution of the end groups as compared to the noninteracting system in dilute solution or due to the fact that the calculated $cm - cm$ total correlation function is not in exact agreement with the experimental data as is apparent from sample S_4 . However, possible deformations of the dendrimers are very weak as compared to the abovementioned linear macromolecules. For comparison we note that a computer simulation study has also revealed only very small deformations of flexible dendrimers, i.e., the overall size of those dendrimers decreases by less than 2 % upon increasing the volume fraction from infinite dilution to the overlap volume fraction.²¹ Thus, we conclude that even in the range of the overlap concentration the dendrimers preserve their structure.

Finally the results shown in Fig. 3 and 4 demonstrate that the decoupling approximation [Eq. (9)] may be used as a first approximation although the height of the calculated peak of the scattering intensity at $q \approx 1.85 \text{ nm}^{-1}$ for sample S_4 is slightly higher than the experimental data. A similar overestimation of the height of such peaks has already been observed by comparing the results of the

decoupling approximation with exact evaluations of the scattering intensity as obtained from a computer simulation study of monodisperse dendrimers.²¹

V. SUMMARY

A general analysis of the scattering intensities of a binary mixture of dissolved dendrimers obtained by small-angle neutron scattering has been presented. Partially deuterated dendrimers [Fig. 1 (B)] have been mixed with the same but protonated dendrimers [Fig. 1 (A)] in dimethylacetamide which is a good solvent for this system. Contrast variation has been used in order to obtain partial scattering intensities allowing one to investigate both the structure and the interaction of dendrimers in concentrated solution. An interpretation of the partial scattering intensities leads to the conclusion that the overall structure of both dendrimers is identical and an appreciable number of end groups must fold back into the interior of the dendrimers in dilute solution [Fig. 2].

Binary dendrimer mixtures have been investigated at various contrasts [Table I] in order to distinguish the influence of the shape of individual dendrimers from the influence of intermolecular interactions on the scattering intensities at high concentrations. The samples S_1 and S_3 provide nearly direct information about the shape of the dendrimers at high concentration. An analysis of the measured scattering intensities for both samples [Figs. 3 and 4] has revealed that the shape of the dendrimers is virtually independent of the concentration. Hence, the flexible poly(propyleneamine) dendrimers of fourth generation have to be considered as shape-persistent molecules within the present limits of approximation. The samples S_2 and S_4 allows one to study the mutual interaction between the dendrimers at two different concentrations. A comparison of the measured scattering intensities with the calculated ones [Figs. 3 and 4] demonstrate that the center-of-mass Ornstein-Zernike relations [Eq. (12)] together with the hypernetted chain closure [Eq. (15)] and the Gaussian interaction potential [Eq. (16)] may be used as a good approximation although the height of the calculated peak of the scattering intensities are slightly higher than the experimental data.

VI. ACKNOWLEDGEMENT

The authors thank the Institute Laue-Langevin in Grenoble (France) for providing beamtime at the Instrument D11.

* E-mail: harnau@fluids.mpi-stuttgart.mpg.de

¹ M. Fischer and F. Vögtle, *Angew. Chem. Int. Ed.* **38**, 884 (1999).

² E. W. Meijer and M. H. P. van Genderen, *Nature (London)* **426**, 128 (2003).

³ M. Ballauff and C. N. Likos, *Angew. Chem. Int. Ed.* **43**,

- 998 (2004).
- ⁴ D. A. Tomalia, *Chem. Today* **23**, 41 (2005).
 - ⁵ W. Krause, N. Hackmann-Schlichter, F. K. Maier, and R. Müller, *Top. Curr. Chem.* **210**, 261 (2000).
 - ⁶ C. A. S. Regino, S. Walbridge, M. Bernardo, K. J. Wong, D. Johnson, R. Lonser, E. H. Oldfield, P. L. Choyke, and M. W. Brechbiel, *Contrast Media Mol. Imaging* **3**, 2 (2008).
 - ⁷ T.-H. Kwon, M. K. Kim, J. Kwon, D.-Y. Shin, S. J. Park, C.-L. Lee, J.-J. Kim, and J.-I. Hong, *Chem. Mater.* **19**, 3673 (2007).
 - ⁸ D. Shabat, R. J. Amir, A. Gopin, N. Pessah, and M. Shamis, *Chem. Eur. J.* **10**, 2626 (2004).
 - ⁹ A. Agarwal, A. Asthana, U. Gupta, and N. K. Jain, *J. Pharm. Pharmacol.* **60**, 671 (2008).
 - ¹⁰ S. Rosenfeldt, N. Dingenouts, M. Ballauff, N. Werner, F. Vögtle, and P. Lindner, *Macromolecules* **35**, 8098 (2002).
 - ¹¹ S. Rosenfeldt, N. Dingenouts, M. Ballauff, P. Lindner, C. N. Likos, N. Werner, and F. Vögtle, *Macromol. Chem. Phys.* **203**, 1995 (2002).
 - ¹² N. Dingenouts, S. Rosenfeldt, N. Werner, F. Vögtle, P. Lindner, A. Roulamo, K. Rissanen, and M. Ballauff, *J. Appl. Cryst.* **36**, 674 (2003).
 - ¹³ S. Rosenfeldt, N. Dingenouts, D. Pötschke, M. Ballauff, A. J. Berresheim, K. Müllen, and P. Lindner, *Angew. Chem. Int. Ed.* **43**, 109 (2004).
 - ¹⁴ S. Rosenfeldt, N. Dingenouts, D. Pötschke, M. Ballauff, A. J. Berresheim, K. Müllen, P. Lindner, and K. Saalwächter, *J. Lumin.* **111**, 225 (2005).
 - ¹⁵ S. Rosenfeldt, E. Karpuk, M. Lehmann, H. Meier, P. Lindner, L. Harnau, and M. Ballauff, *ChemPhysChem* **7**, 2097 (2006).
 - ¹⁶ C. N. Likos, M. Schmidt, H. Löwen, M. Ballauff, D. Pötschke, and P. Lindner, *Macromolecules* **34**, 2914 (2001).
 - ¹⁷ C. N. Likos, S. Rosenfeldt, N. Dingenouts, M. Ballauff, P. Lindner, N. Werner, and F. Vögtle, *J. Chem. Phys.* **117**, 1869 (2002).
 - ¹⁸ I. O. Götze and C. N. Likos, *Macromolecules* **36**, 8189 (2003).
 - ¹⁹ H. M. Harreis, C. N. Likos and M. Ballauff, *J. Chem. Phys.* **118**, 1979 (2003).
 - ²⁰ I. O. Götze, H. M. Harreis, and C. N. Likos, *J. Chem. Phys.* **120**, 7761 (2004).
 - ²¹ I. O. Götze and C. N. Likos, *J. Phys.: Condens. Matter* **17**, S1777 (2005).
 - ²² I. O. Götze, A. J. Archer, and C. N. Likos, *J. Chem. Phys.* **124**, 084901 (2006).
 - ²³ C. N. Likos, B. M. Mladek, D. Gottwald, and G. Kahl, *J. Chem. Phys.* **126**, 224502 (2007).
 - ²⁴ T. Terao, *Chem. Phys. Lett.* **446**, 350 (2007).
 - ²⁵ T. Terao, *J. Appl. Cryst.* **40**, s581 (2007).
 - ²⁶ L. Harnau, S. Rosenfeldt, and M. Ballauff, *J. Chem. Phys.* **127**, 014901 (2007).
 - ²⁷ B. M. Mladek, G. Kahl, and C. N. Likos, *Phys. Rev. Lett.* **100**, 028301 (2008).
 - ²⁸ S. Uppuluri, S. E. Keinath, D. A. Tomalia, and P. R. Dvornic, *Macromolecules* **31**, 4498 (1998).
 - ²⁹ A. Topp, B. J. Bauer, T. J. Prosa, R. Scherrenberg and E. J. Amis, *Macromolecules* **32**, 8923 (1999).
 - ³⁰ I. Bodnar, A. S. Silva, R. W. Deitcher, N. E. Weisman, Y. H Kim, and N. J. Wagner, *J. Poly. Sci. Part B* **38**, 857 (2000).
 - ³¹ A. I. Sagidullin, A. M. Muzafarov, M. A. Krykin, A. N. Ozerin, V. D. Skirda, and G. M. Ignat'eva, *Macromolecules* **35**, 9472 (2002).
 - ³² A. Lang, C. N. Likos, M. Watzlawek, and H. Löwen, *J. Phys.: Condens. Matter* **12**, 5087 (2000).
 - ³³ M. Daoud, J. P. Cotton, B. Farnoux, G. Jannink, G. Sarma, H. Benoit, R. Duplessix, C. Picot, and P. G. de Gennes, *Macromolecules* **8**, 804 (1975).
 - ³⁴ A. Yethiraj and C. K. Hall, *J. Chem. Phys.* **96**, 797 (1992).
 - ³⁵ S. Bolisetty, C. Airaud, Y. Xu, A. H. E. Müller, L. Harnau, S. Rosenfeldt, P. Lindner, and M. Ballauff, *Phys. Rev. E* **75**, 040803(R) (2007).
 - ³⁶ S. Bolisetty, S. Rosenfeldt, C. N. Rochette, L. Harnau, P. Lindner, Y. Xu, A. H. E. Müller, and M. Ballauff, *Colloid. Polym. Sci.* **287**, 129 (2009).
 - ³⁷ M. J. Stevens and K. Kremer, *Phys. Rev. Lett.* **71**, 2228 (1993).
 - ³⁸ A. Yethiraj, *Phys. Rev. Lett.* **78**, 3789 (1997).
 - ³⁹ Y. Xu, S. Bolisetty, M. Drechsler, B. Fang, J. Yuan, L. Harnau, M. Ballauff, and A. H. E. Müller, *Soft Matter* **5**, 379 (2009).
 - ⁴⁰ L.-T. Yan, Y. Xu, M. Ballauff, A. H. E. Müller, and A. Böker, *J. Phys. Chem. B* **113**, 5104 (2009).
 - ⁴¹ M. Ballauff and Y. Lu, *Polymer* **48**, 1815 (2007).
 - ⁴² S. Bolisetty, M. Hoffmann, Th. Hellweg, M. Ballauff, and L. Harnau, *Macromolecules* **42**, 1264 (2009).
 - ⁴³ J. S. Higgins and H. C. Benoît, *Polymers and Neutron Scattering*, (Clarendon Press Oxford, New York, 1994).
 - ⁴⁴ H. Stephan, H. Spies, B. Johannsen, L. Klein, and F. Vögtle, *Chem. Commun.* **18**, 1875 (1999).
 - ⁴⁵ P. Lindner, R. P. May, and P. A. Timmins, *Physica B* **180-181**, 967 (1992).
 - ⁴⁶ K. Lieutenant, P. Lindner, and R. Gähler, *J. Appl. Cryst.* **40**, 1056 (2007).
 - ⁴⁷ K. S. Schweizer and J. G. Curro, *Adv. Chem. Phys.* **98**, 1 (1997).
 - ⁴⁸ L. Harnau, *Molec. Phys.* **106**, 1975 (2008).
 - ⁴⁹ A. Yethiraj, *J. Phys. Chem. B* **113**, 1539 (2009).
 - ⁵⁰ A. Yethiraj and C.-Y. Shew, *Phys. Rev. Lett.* **77**, 3937 (1996).
 - ⁵¹ L. Harnau, *J. Chem. Phys.* **115**, 1943 (2001).
 - ⁵² C.-Y. Shew and A. Yethiraj, *J. Chem. Phys.* **109**, 5162 (1998).
 - ⁵³ L. Harnau and J.-P. Hansen, *J. Chem. Phys.* **116**, 9051 (2002).
 - ⁵⁴ L. Harnau and P. Reineker, *J. Chem. Phys.* **112**, 437 (2000).
 - ⁵⁵ L. Harnau, D. Costa, and J.-P. Hansen, *Europhys. Lett.* **53**, 729 (2001).
 - ⁵⁶ C. H. M. Weber, A. Chiche, G. Krausch, S. Rosenfeldt, M. Ballauff, L. Harnau, I. Göttker-Schnetmann, Q. Tong, and S. Mecking, *Nano Letters* **7**, 2024 (2007).
 - ⁵⁷ K. Henzler, S. Rosenfeldt, A. Wittemann, L. Harnau, T. Narayanan, and M. Ballauff, *Phys. Rev. Lett.* **100**, 158301 (2008).
 - ⁵⁸ V. Krakoviack, J.-P. Hansen, and A. A. Louis, *Europhys. Lett.* **58**, 53 (2002).